Accurate numerical modeling of convective heat transfer coefficient for a high power PLA-core toroidal electromagnetic coupler subject to cooling

Fatima Zahra Boudara, Hajar Bouzekri, Y. Benhammadi, Pierre-Henri Cocquet, Marc Rivaletto, Laurent Pecastaing, Antoine Silvestre de Ferron, Yves Le Guer

International Journal of Thermal Sciences 170 (2021) 107125

Contents lists available at ScienceDirect

International Journal of Thermal Sciences

journal homepage: www.elsevier.com/locate/ijts

Accurate numerical modeling of convective heat transfer coefficient for a high power PLA-core toroidal electromagnetic coupler subject to cooling

F.Z. Boudara [a,*], H. Bouzekri [a], Y. Benhammadi [a], P.-H. Cocquet [b,a], M. Rivaletto [a], L. Pécastaing [a], A. Silvestre de Ferron [a], Y. Le Guer [a]

[a] Laboratoire des Sciences de l'Ingénieur Appliquées à la Mécanique et au Génie Electrique – Fédération IPRA, Université de Pau et des Pays de l'Adour/E2S UPPA, 64000 Pau, France

[b] Laboratoire de Physique et Ingénierie Mathématique pour l'Énergie et l'Environnement (PIMENT), Université de la Réunion, Sainte-Clotilde, France

ARTICLE INFO

Keywords:
Electromagnetic coupler
Torus
Convective cooling

ABSTRACT

The toroidal electromagnetic coupler has many advantages over the classical transformer. It is widely used in low-power applications. However, there are some limits that hamper its use in modern and high-power applications, such as the cost, the difficulty of winding and, especially, the limited number of studies carried out on the thermal aspect. In this article, we look at the problem of cooling a high-power and very compact toroidal electromagnetic coupler used in smart grid systems. The cooling is modeled thanks to heat transfer coefficients considering the windings as a surface heat source. A mathematical model which is quick and useful for a first approach is developed, and the results obtained show the temperature distribution for convective boundary conditions inside and outside the hollow torus. In addition, a parametric study is carried out. It aims to determine the optimal internal and external convective heat transfer coefficients for which the temperature of the coupler remains below the material's destruction threshold. Additionally, a 3D numerical model taking into account the wires of the toroidal coupler is studied and compared with the mathematical model. The good consistency between the two methods ensures that this simplified thermal modeling can be trusted for the study of thermal management during the design of future electromagnetic couplers.

1. Introduction

The increase in greenhouse gases observed in recent decades, mainly caused by non-renewable energy sources, has led to a rise in renewable ones such as solar, wind, or fuel cell energies. For their implementation, these sources require mastery of the power they deliver through adequate and intelligent flow management. In particular, the fast charging of autonomous systems will lead to the transfer of electrical power which is far greater than the capacities of the products currently on the market [1].

With this in mind, compact toroidal electromagnetic couplers with a circular cross-section were developed [2]. An example is presented in Fig. 1. The primary and secondary windings wound over the entire surface of the torus confine the magnetic field, offering the toroidal coupler very reduced electromagnetic radiation. It also has advantages related to size and volume. Thanks to these qualities, it is widely used in low-power applications such as public lighting, or even in the production of current or voltage sources with a very low internal resistance. However, the toroidal electromagnetic coupler is still not widely available in high-power applications and has been studied less than the conventional transformer.

The electromagnetic coupler proposed here has the particularity of not using any magnetic materials (not even ferrite bars to better confine the magnetic field). To simplify its use in high-power applications and retain its compactness, the magnetic core of the coupler was removed in order to avoid magnetic losses. The only losses the system has are Joule losses due to the AC resistance of the Litz wire used in the design of the prototype. The core of the coupler was replaced by a polymer material, used only as a mount for the cable windings. Additionally, to prevent a high additional eddy current loss, the use of metals for the cable holder is not permitted. Therefore, PLA material was chosen to support the 3D-printed cable holder because of its ease of use, low-loss tangent and high-volume resistivity. However, this material is not feasible from a thermomechanical point of view because of its temperature limit, which must not exceed (60 °C), forcing the torus coupler to be cooled down. The PLA cable holder was thus manufactured using a filament 3D printer, as shown in Fig. 1. The printable volume did not allow the cable holder to be printed in one piece, so we had to make it in

* Corresponding author.
E-mail address: fatima-zahra.boudara@univ-pau.fr (F.Z. Boudara).

https://doi.org/10.1016/j.ijthermalsci.2021.107125
Received 9 January 2021; Received in revised form 22 May 2021; Accepted 7 June 2021
Available online 6 July 2021

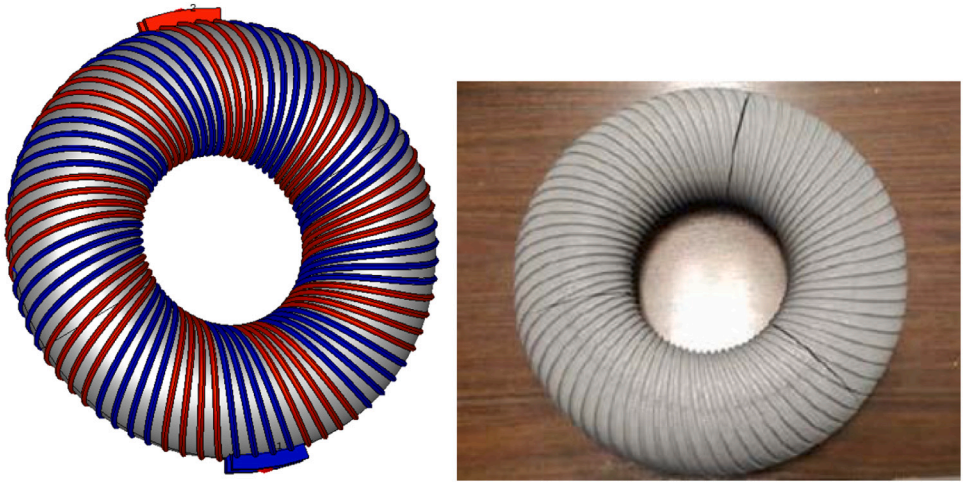

Fig. 1. The toroidal electromagnetic coupler. The primary winding and its electrical connection for the four parallel wires are represented by the color red. The secondary winding and its electrical connection are represented by the color blue. The gray part is the PLA cable holder. Right: The 3D printed PLA cable holder.

Table 1
Thermophysical properties of PLA [3].

Property	Value	Unit
Solid density ρ	1300	kg m^{-3}
Heat capacity Cp	1800	J kg^{-1} K^{-1}
Thermal conductivity k	0.13	W m^{-1} K^{-1}
Thermal diffusivity α	5.6 10^{-8}	m^2 s^{-1}

three pieces. The thermophysical properties of PLA (Polylactic Acid) are given in Table 1.

To our knowledge, no plastic-core electromagnetic toroidal coupler studies have been reported in the scientific literature to date, either for low-power or high-power applications. Our work is therefore the first thermal preliminary study of a high-power electromagnetic toroidal coupler.

In this paper, we chose to model natural or forced convection with constant heat transfer coefficients. We are aware that this is a strong approximation. But as we did not initially know which technical solution would be used and how the flows would be directed to the surfaces of the torus to be cooled, we chose this solution. Depending on the direction of the flow approaching the external torus surface, different vortex structures may develop downstream, and a vortex shedding with a certain frequency may appear [4,5]. These spatially complex and unsteady flows will therefore imply a local dependence of the convective coefficients on the azimuthal and poloidal directions (cf. Fig. 5) which have barely been studied to date [6–8]. Inside the torus, the convective flows will develop in the well-known form of Dean's counter-rotating helical cells [9], which develop within flat (torsion-free) channels of constant curvature (here R). They will also induce variations in the azimuthal and poloidal directions of the convective transfer coefficients [10,11]. Thus, due to the complexity of the internal and external flow situations that can exist depending on the flow and convection regimes (natural or forced), in this work we chose to use constant mean convective exchange coefficients for the external exchange surface h_{ext} and also for the internal exchange surface h_{int}.

To study the thermal management of the torus, we first carried out mathematical thermal modeling of the electromagnetic coupler. For simplicity, the heat generated by the Joule effect from the primary and secondary windings is understood as a dissipated heat flux on the boundary of the PLA holder (see Fig. 1). Consequently, the coupler can be considered only as a hollow torus which is subjected to a parietal heat flux (the Joule losses) and to external and internal convective cooling with fluid inlet and outlet.

As previously mentioned, the heat transfer problem in a hollow torus with convective boundary conditions has never been studied in the literature, either analytically or numerically. The only works we found for heat transfer within a torus are those of Wiesche [12] Alassar and Abushoshah [13,14] but they concern other types of boundary conditions.

We relied on numerical simulations only to compute the temperature distribution inside the torus. Since we wished to know whether the temperature inside the PLA holder rises above 60°C, we computed the optimal internal and external convective heat transfer coefficients for which the PLA holder is not deteriorated. The optimization was performed parametrically, meaning that only one parameter (e.g. internal or external temperature, minor or major radius, etc.) varied, while the others remained fixed.

It should be emphasized that the previous model approximates the windings as a surface source term. We did not consider the complete geometry of the electromagnetic coupler. It was therefore of interest to compute the temperature inside the coupler while also considering the primary and secondary windings. To achieve this, numerical simulations using ANSYS-Fluent were performed. We used the optimal value of the external heat transfer coefficients obtained with the first modeling to compare the two approaches.

It is worth remembering that this article proposes a preliminary and simplified study of the thermal management of toroidal couplers. This study gives an easy and quick idea of the maximum temperature of the system for different levels of power losses as well as for different dimensions of the toroidal coupler. Among the main objectives of the project is the continuous optimization of the coupler; for this, other toroidal couplers which are more compact than the one presented in this article are under development. Studying their thermal feasibility is a radical point in our optimization process.

Our paper is organized as follow: we first introduce the characteristics of the toroidal electromagnetic coupler and the electrical experimental tests to identify the heat flux to be cooled. Next, the thermal modeling of the torus subjected to external convective boundary conditions with a dissipated heat flux is proposed. In the third section, the complete geometry with the winding is taken into account. The thermal and 3D numerical models are then compared and discussed. Finally, the paper ends with some conclusions and future avenues for research.

2. The system's electrical performances

This section is dedicated to the presentation of the characteristics and the electrical performances of the electromagnetic coupler. The

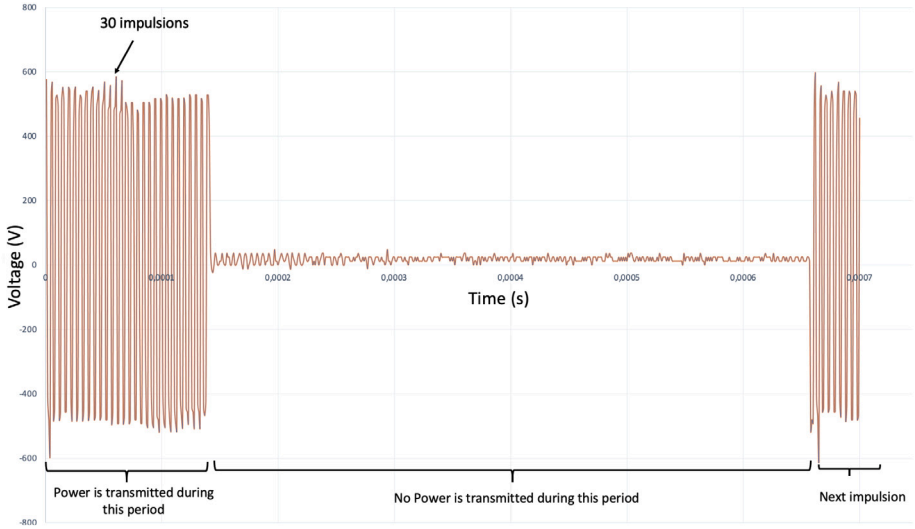

Fig. 2. Experimental waveform of the input voltage in burst regime.

operating regime of the system is also explained in full in order to provide a better understanding of the usefulness of studying the thermal management of the toroidal coupler.

2.1. Operating regime

Before developing a cooling system for the electromagnetic coupler, the electrical performances of the system must be checked. For this reason, the only way to test the toroidal coupler at a high-power level without damaging it is to use burst mode. In this regime, the system works only for a very short period and stops for a long time before the next cycle. Consequently, the system does not have enough time to heat up.

Fig. 2 shows the waveforms of the input voltage while the system is working in burst regime. The first part of the signal is made up of several pulses (here, 30). The system operates only during this period (0.25% of the time) and no power is transmitted otherwise. This signal is repeated every 0.65 ms.

By adopting this operating regime, the electrical performance of the toroidal coupler can be evaluated. The dissipated heat flux can also be determined experimentally in order to study analytically and/or numerically the temperature rise at high power as well as the various possible cooling solutions. However, to confirm these results through experimental measurements, it is first mandatory to develop a cooling system and to operate it continuously, as shown in Fig. 3.

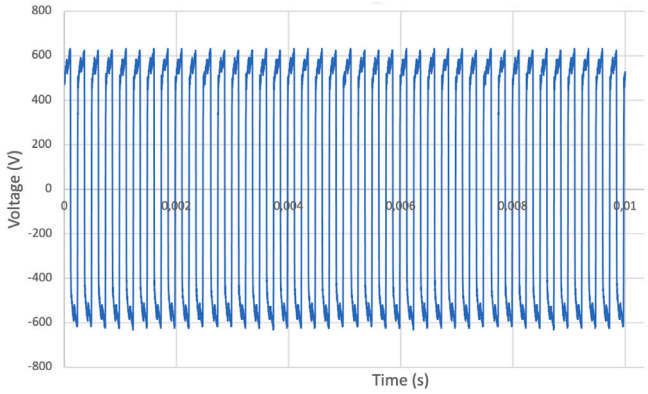

Fig. 3. Experimental waveform of the input voltage in continuous regime. The project's ultimate goal is for the electromagnetic coupler to operate continuously throughout the period, so a cooling system is mandatory to avoid the PLA cable holder melting.

Table 2
Parameters of the electromagnetic coupler [2].

Parameter	Value	Unit
R	124	mm
r_2	52.25	mm
r_1	26.12	mm
Frequency	200	kHz
R_{AC}	15	mΩ

2.2. Characteristics of the toroidal electromagnetic coupler

The electromagnetic coupler's parameters are presented in Table 2. The cable holder is hollow, so the inner radius of the tube is r_1, the outer radius of the tube is r_2 and R is the torus radius.

To ensure the compactness of the electromagnetic coupler, a high operating frequency of 200 kHz is used. Working at such a frequency level requires limiting AC losses due to the skin and proximity effects. Therefore, a Litz wire composed of 2500 strands with 71 μm diameters is used according to the operating frequency. At this frequency, the measured AC resistances R_{AC} of the primary and secondary windings of the electromagnetic coupler are 15 mΩ.

Fig. 4 presents the experimental setup. The measured average transmitted power is almost 200 kW with an efficiency of 97.7%. The primary current (I_{1rms}) is measured to be 400 A and the secondary current(I_{2rms}) is 373 A. According to:

$$P_{losses} = R_{AC} I_{1rms}^2 + R_{AC} I_{2rms}^2,$$

the primary losses are 2.4 kW and the secondary losses are 2.1 kW, so total AC losses measured for this operating point come to 4.5 kW. Therefore, the thermal study is carried out in a steady state mode considering a heat flux of 4.5 kW to be cooled.

Therefore, the thermal study will be carried out in a steady state mode considering a heat flux of 4.5 kW to be cooled.

3. Cooling a torus: thermal modeling

The first part of this section presents the geometrical parametrization of a hollow torus by the poloidal coordinates. Next, the heat equation with convective boundary conditions is presented. The third part is dedicated to the parametric optimization study giving the optimal heat transfer coefficients for which the PLA holder is not deteriorated. Finally, the numerical results are discussed, including the temperature distribution inside the toroidal coupler.

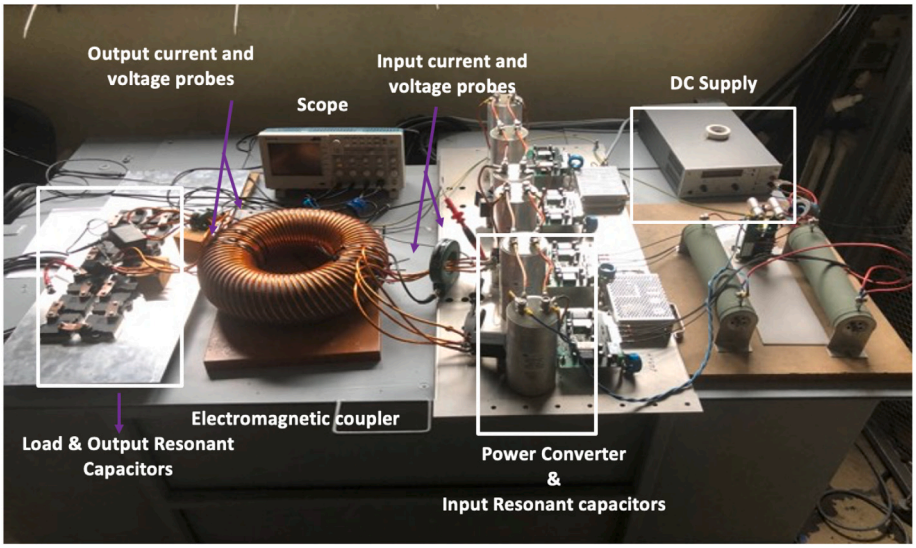

Fig. 4. The experimental setup. The DC source supplies the system with DC voltage, then the power converter (developed by our industrial partner EFFITECH) converts the DC voltage to AC voltage at the input of the electromagnetic coupler. The resonant capacitors are used to compensate for the inductive effect of the primary side and enhance the power capability transfer. The current and voltage probes are used to measure the input and output current and voltage, enabling us to determine the average input and output power. The scope is used to show the waveforms of the input and output current and voltage signals. A resistive load of 1 Ω is used at the output of the electromagnetic coupler.

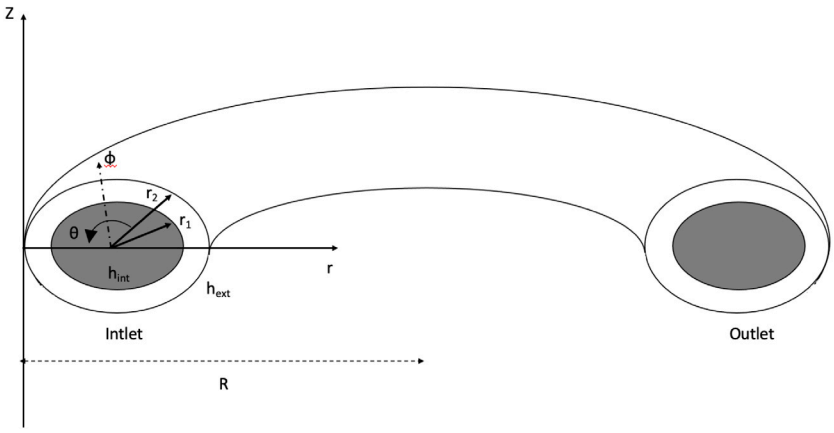

Fig. 5. Parametrization of a torus by the coordinates (r, θ, ϕ).

3.1. Geometrical parametrization

The parametrization of a hollow torus is (cf. Fig. 5) as follow :

$$\begin{cases} x(r,\theta,\phi) &= (R + r\cos(\theta))\cos(\phi), \\ y(r,\theta,\phi) &= (R + r\cos(\theta))\sin(\phi), \\ z(r,\theta,\phi) &= r\sin(\theta), \end{cases} \tag{1}$$

where R is the radius of the tore, $r_1 \leq r \leq r_2$ is the radius of the tube, R/r is the aspect ratio, θ and ϕ are the angles in the poloidal and toroidal directions, respectively, with $(\theta, \phi) \in [0, 2\pi] \times [0, 2\pi]$. For a torus with minor radius r, its surface is

$$S_{torus} = 4\pi^2 Rr, \tag{2}$$

and its volume is

$$V_{torus} = 2\pi^2 Rr^2. \tag{3}$$

For a hollow torus with inner and outer radius r_1 and r_2, its volume can be computed from (3) and reads

$$V_{hollow-torus} = 2\pi^2 R\left(r_2^2 - r_1^2\right). \tag{4}$$

3.2. Heat equation with convective boundary conditions

The transient heat conduction equation to solve is:

$$\Delta T = \frac{1}{\alpha}\frac{\partial T}{\partial t} \tag{5}$$

where T is the temperature, α is the thermal diffusivity of the material, and t is the time. We first rewrite the heat equation in the (r, θ, ϕ) coordinates. The metric tensor is defined as $g = J^T J$ where J is the Jacobian matrix of the mapping $(r, \theta, \phi) \mapsto (x, y, z)$. Some computations give

$$g = \begin{pmatrix} 1 & 0 & 0 \\ 0 & r^2 & 0 \\ 0 & 0 & (R + r\cos(\theta))^2 \end{pmatrix}, \quad g^{-1} = \begin{pmatrix} 1 & 0 & 0 \\ 0 & \frac{1}{r^2} & 0 \\ 0 & 0 & \frac{1}{(R+r\cos(\theta))^2} \end{pmatrix}.$$

As a result, denoting $(g^{ij})_{ij} = g^{-1}$, the Laplace operator in the moving frame reads (we use the summation over repeated indices and refer to [15] for the differential operators associated with a metric tensor)

$$\begin{aligned} \widetilde{\Delta} f &= \frac{1}{\sqrt{g}}\partial_j\left(\sqrt{g}g^{jk}\partial_k f\right) \\ &= \frac{1}{\sqrt{g}}\left(\partial_r\left(\sqrt{g}\partial_r f\right) + \partial_\theta\left(\frac{\sqrt{g}}{r^2}\partial_\theta f\right) + \partial_\phi\left(\frac{\sqrt{g}}{(R + r\cos(\theta))^2}\partial_\phi f\right)\right), \end{aligned}$$

where $\sqrt{g} = r(R + r\cos(\theta))$ is the square root of the determinant of the metric tensor. The transient heat equation (5) is then transformed into (r, θ, ϕ) coordinates as follows

$$\widetilde{\Delta T} = \frac{1}{\alpha}\frac{\partial \widetilde{T}}{\partial t}, \tag{6}$$

where $\widetilde{T}(t, r, \theta, \phi) = T(t, x, y, z)$ is the temperature in the (r, θ, ϕ) coordinates.

We consider a hollow torus of respectively inner radius r_1 and outer radius r_2 of the toroidal tube. The torus is to be air or water-cooled, by convection (natural or forced) inside the torus (h_{int}) and air-cooled outside the torus (h_{ext}) (see Fig. 5). As a first approach, we will consider the constant convective heat exchange coefficients as explained above. The temperatures of the fluid inside and outside the torus are respectively T_{int} and T_{ext}. We recall that the Litz wires are considered as a surface heat source. The heat flux Q dissipated by the Litz wires is considered to be homogeneously distributed at the outer surface of the toroidal tube S_{ext}, where $S_{\text{ext}} = 4\pi^2 r_2 R$ (see (2)). Taking into account the convective heat flux with the Fourier law, the boundary conditions finally reads as follows:

$$\begin{aligned} r = r_2 :\ & -k\frac{\partial \widetilde{T}}{\partial r}\bigg|_{r=r_2} = -\frac{Q}{S_{\text{ext}}} + h_{\text{ext}}\left(\widetilde{T}|_{r=r_2} - T_{\text{ext}}\right), \\ r = r_1 :\ & k\frac{\partial \widetilde{T}}{\partial r}\bigg|_{r=r_1} = h_{\text{int}}\left(\widetilde{T}|_{r=r_1} - T_{\text{int}}\right), \end{aligned} \tag{7}$$

where k is the thermal conductivity of the material.

We now give the dimensionless form of the previous heat equation. To do so, we introduce the aspect ratio of the torus η and the dimensionless quantities

$$\eta = \frac{R}{b},\ t^* = \frac{t}{t_0} = \frac{\alpha t}{b^2},\ r^* = \frac{r}{b},$$

where t_0 and b are arbitrary. Using the notation $f^*(t^*, r^*, \theta, \phi) = f(t/t_0, r/b, \theta, \phi)$, we get

$$\frac{\partial f^*}{\partial r^*} = b\frac{\partial f}{\partial r},\ \frac{\partial f^*}{\partial t^*} = \frac{b^2}{\alpha}\frac{\partial f}{\partial t}.$$

The dimensionless Laplace operator now reads

$$\begin{aligned} \widetilde{\Delta}^* f^* = & \frac{1}{b^2}\left(\frac{\partial^2 f^*}{\partial r^{*2}} + \frac{1}{(r^*)^2}\frac{\partial^2 f^*}{\partial \theta} + \frac{1}{(\eta + r^*\cos(\theta))^2}\frac{\partial^2 f^*}{\partial \phi^2}\right) \\ & + \frac{1}{b^2}\left(\frac{2r^*\cos(\theta) + \eta}{r^*(\eta + r^*\cos(\theta))}\frac{\partial f^*}{\partial r^*} - \frac{1}{(r^*)^2}\frac{r^*\sin(\theta)}{(\eta + r^*\cos(\theta))}\frac{\partial f^*}{\partial \theta}\right). \end{aligned}$$

We also introduce the notation $\widetilde{\Delta}^* f^* = \frac{1}{b^2}\mathcal{L}^*[f^*]$ and the following dimensionless temperature

$$T^*(t^*, r^*, \theta, \phi) = \frac{T\left(\frac{t}{t_0}, \frac{r}{b}, \theta, \phi\right) - T_\infty}{T_{\text{ref}}},$$

where T_∞ and T_{ref} are arbitrary. The dimensionless heat equation is then

$$\frac{\partial T^*}{\partial t^*} = \mathcal{L}^*[T^*].$$

Denoting $r_1^* = r_1/b$ and $r_2^* = r_2/b$, the boundary conditions are recast into

$$\begin{aligned} r^* = r_2^* :\ & -\frac{\partial T^*}{\partial r^*}\bigg|_{r^*=r_2^*} = -Q^* + Bi_{\text{ext}}\left(T^*|_{r^*=r_2^*} + \frac{T_\infty - T_{\text{ext}}}{T_{\text{ref}}}\right), \\ r^* = r_1^* :\ & \frac{\partial T^*}{\partial r^*}\bigg|_{r^*=r_1^*} = Bi_{\text{int}}\left(T^*|_{r^*=r_1^*} + \frac{T_\infty - T_{\text{int}}}{T_{\text{ref}}}\right), \end{aligned}$$

where

$$Q^* = \frac{Q\,b}{kT_{\text{ref}}S_{\text{ext}}}$$

is the dimensionless surface heat source and

$$Bi_{\text{int}} = \frac{h_{\text{int}}\,b}{k},\ Bi_{\text{ext}} = \frac{h_{\text{ext}}\,b}{k}$$

are the inner and outer Biot numbers. The latter, for example, characterizes the ratio of the heat transfer resistances, conductive inside the body and convective at the external boundary of the torus. Above b is a characteristic length defined by the ratio of the volume to the surface of the body at the surface in question, namely $r = r_2$:

$$b = \frac{1}{2\pi}\frac{r_2^2 - r_1^2}{r_2}. \tag{8}$$

We recall that the temperature inside the torus does not depend on the spatial variable (i.e. lumped analysis) if $Bi < 0.1$. In our case, this yields

$$h < \frac{0.1\,k}{b} = 0.664,$$

which indicates that the lumped analysis does not apply to our torus when natural convection or forced convection is involved. We thus rely on numerical simulations to get the temperature inside the torus.

3.3. Numerical method

Recall that the electromagnetic coupler is intended to operate continuously. The coupler reaches its maximal temperature in the steady-state regime. Since this is the most difficult case related to cooling, we are now working in the steady regime. We can consider that the heat flux that emanates from the torus wall is transferred to the cooling fluid that flows inside the torus. Thus, if we consider the assumption of a steady flow, along a differential element dx of the inner torus channel, the fluid will undergo a temperature variation dT_m which can be calculated by knowing the heat flow transferred to the wall dq:

$$dq = m\,C_p\,dT_m = q_s''\,P\,dx$$

where m is the constant flow rate of the fluid, C_p its specific heat, P is the inner surface perimeter of the torus and q_s'' is the inner surface heat flux density.

Since no explicit solution can be found in the setting considered, numerical simulation is then used to compute the temperature inside the torus slice (a differential element dx). The conduction problem is solved using finite elements and Free-Fem ++ [16]. Let $\mathcal{T}$ be a quasi-uniform triangular mesh of $[0, 1] \times [0, 2\pi]$ and

$$\mathbb{X}_\tau = \left\{\psi_\tau \text{ is continuous} \mid \psi_\tau|_T \in \mathbb{P}_1 \text{ and } \theta \mapsto \psi_\tau(r, \theta)\ 2\pi\text{-periodic}\right\}.$$

Let τ_T be the diameter of its inscribed circle. The meshsize τ is then defined as $\tau = \max_{T\in\mathcal{T}} \tau_T$. The variational formulation of (6)–(7) is obtained by multiplying (6) with a test function $\sqrt{g}\varphi$, integrating by part and then using the boundary condition (7) (see [17, Chapter IX]). The discretized variational formulation of (6)–(7) then reads:

Find $T_\tau \in \mathbb{X}_\tau$ satisfying

$$\begin{aligned} & \int_{r=0}^{1}\int_{\theta=0}^{2\pi}\left(\partial_r T_\tau \partial_r \varphi_\tau + \frac{1}{r^2}\partial_\theta T_\tau \partial_\theta \varphi_\tau\right)\sqrt{g}\,dr\,d\theta \\ & + \int_{\theta=0}^{\theta=2\pi}\frac{h_{\text{ext}}}{k}\left(\sqrt{g}T_\tau\varphi_\tau\right)\Big|_{r=r_2} + \frac{h_{\text{int}}}{k}\left(\sqrt{g}T_\tau\varphi_\tau\right)\Big|_{r=r_1}\,d\theta \\ & - \int_{\theta=0}^{2\pi}\left(\sqrt{g}\varphi_\tau\right)\Big|_{r=r_2}\left(\frac{Q}{kS_{\text{ext}}} + \frac{h_{\text{ext}}}{k}T_{\text{ext}}\right) + \left(\sqrt{g}\varphi_\tau\right)\Big|_{r=r_1}\frac{h_{\text{int}}}{k}T_{\text{int}}\,d\theta \\ & = \int_{r=r_1}^{r_2}\int_\theta \sqrt{g}F\varphi_\tau\,dr\,d\theta,\ \forall\varphi_\tau \in \mathbb{X}_\tau. \end{aligned} \tag{9}$$

where F is a volume source term set to zero in the following numerical results.

3.4. Parametric optimization in the steady regime

First, we show that cooling the torus so that the PLA is not deteriorated is mandatory. For this purpose, the external and internal heat transfer coefficients are chosen equal to be equal 25 W m^{-2} K^{-1}. Fig. 6 presents the temperature rise at the level of the tube and not the torus, it represents a cross-section of the coupler's loop. For the sake of simplicity, only one half of the tube is presented as there is a symmetry

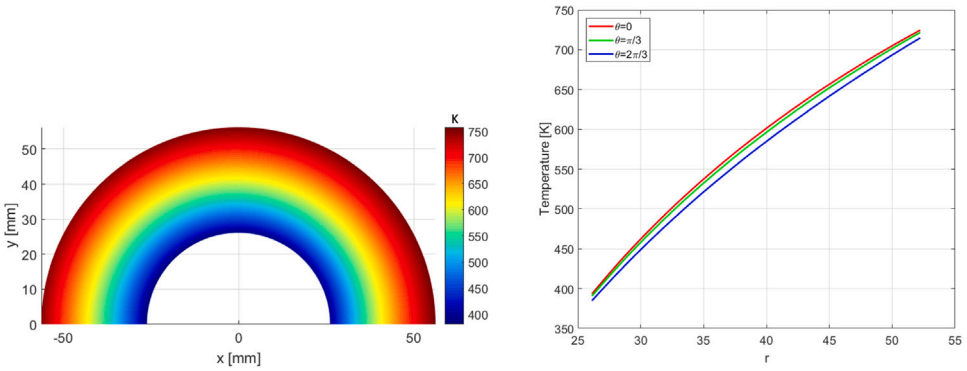

Fig. 6. The temperature rise of the coupler's loop as function of r (mm) with $Q = 5000\,\mathrm{W}$, $h_{\mathrm{ext}} = h_{\mathrm{int}} = 25\ \mathrm{W\ m^{-2}\ K^{-1}}$ with $T_{\mathrm{ext}} = 20\ °\mathrm{C}$. Left: Temperature field. The center of the torus is located on the left. Right: Cut along some angles, $\theta = 0$, $\theta = \pi/3$ and $\theta = 2\pi/3$.

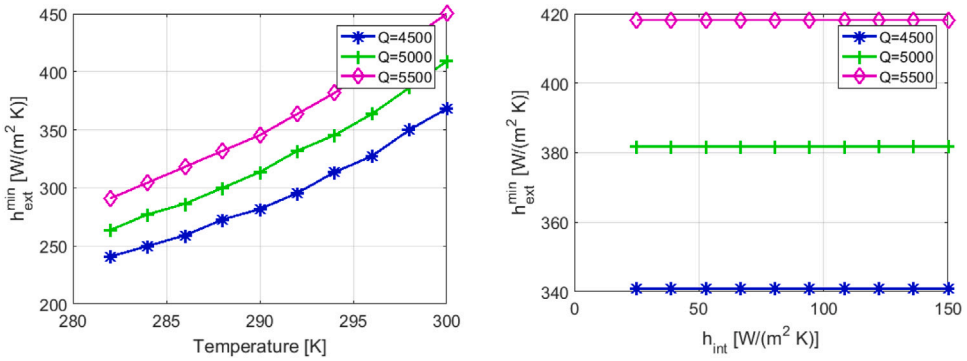

Fig. 7. Value of $h_{\mathrm{ext}}^{\mathrm{min}}$ for the numerical experiments from Table 3 for different values of the heat flux Q (W) dissipated by the Litz wires. Left: Case 1, Right: Case 2.

between the top and the bottom of the tube and also because the convective heat exchange coefficients are considered constant. From this figure, it can be noticed that the temperature is lower at the inner radius of the loop and reaches its maximal value on the outer surface, namely where the flux dissipated by the wires is involved.

Concerning the temperature rise with natural convection, the maximum reached temperature reached is 758 K (485.55 °C). It is obvious that at such a level of heat losses, the temperature rise will be huge and the electromagnetic coupler will need to be cooled down.

Fig. 6 shows the evolution of the temperature at different places. The red curve is when $\theta = 0$, which is at the extremity of the loop, as seen in Fig. 6. The green curve is for $\theta = \pi/3$ and the blue one is for $\theta = 2\pi/3$. This clearly shows that the temperature distribution is not the same at all points of the loop since, in poloidal coordinates, there is no symmetry according to θ. We emphasize that this is the main difference between resolving the system in cylindrical coordinates and in poloidal ones.

In Fig. 6, we can see that the electromagnetic coupler needs larger h to avoid destruction of the material. Next, we numerically compute the minimal value for the external convective heat transfer coefficient h_{ext} for which the PLA does not melt. Let $h_{\mathrm{ext}}^{\mathrm{min}}$ be the minimal value of the external heat transfer coefficient such that the maximal temperature of the torus does not exceed 60°C. The latter is thus defined as

$$h_{\mathrm{ext}}^{\mathrm{min}} = \min\left\{h_{\mathrm{ext}} \text{ such that } \max T < 60°\mathrm{C}\right\},$$

where $\widetilde{T}$ is the temperature computed from the heat equation (6)–(7). Before going further into the parametric optimization, it is worth noting that (6)–(7) can have closed-form solutions when

$$h_{\mathrm{int}} = 0.$$

Indeed, the only solution to (6)–(7) is the constant temperature T, satisfying

$$0 = -\frac{Q}{S_{\mathrm{ext}}} + h_{\mathrm{ext}}\left(T - T_{\mathrm{ext}}\right),$$

Table 3
Investigated configurations for cooling a torus.

	T_{ext} [K]	T_{int} [K]	r_1 [mm]	r_2 [mm]	R [mm]	h_{int} [W m^{-2} K^{-1}]
Case 1	varying	$= T_{\mathrm{ext}}$	26.12	52.25	178.75	25
Case 2	300	300	26.12	52.25	178.75	varying
Case 3	300	300	26.12	varying	178.75	25
Case 4	300	300	26.12	52.25	varying	25

which gives

$$T = \frac{Q}{S_{\mathrm{ext}} h_{\mathrm{ext}}} + T_{\mathrm{ext}}.$$

The value of $h_{\mathrm{ext}}^{\mathrm{min}}$ is thus

$$h_{\mathrm{ext}}^{\mathrm{min}} = \frac{Q}{S_{\mathrm{ext}}(60 - T_{\mathrm{ext}})}. \tag{10}$$

We now compute the value of $h_{\mathrm{ext}}^{\mathrm{min}}$ when $h_{\mathrm{int}} \neq 0$ in the settings given in Table 3.

All the following numerical experiments have been done with the same meshsize $\tau \approx 0.0141$ mm and the numerical results can be found in Fig. 7 for Cases 1–2 and Fig. 8 for Cases 3–4.

From our numerical results, we may draw the following conclusions. First, the value of $h_{\mathrm{ext}}^{\mathrm{min}}$ increases with Q and with the exterior and the interior temperatures (cf. Fig. 7 - Left). In addition, as seen in Fig. 7 (Right), $h_{\mathrm{ext}}^{\mathrm{min}}$ is not affected by the value of the interior heat transfer coefficient, which indicates that it is not worth trying to cool the torus from the inside. We expect that this result to stem from two mains factors. First, the thermal conductivity of the PLA material is small, hence this material is a thermal insulator. In addition, the power is dissipated on the outer surface of the torus. In fact, all the cooling work is done by the external heat transfer coefficient and increasing the internal heat transfer coefficient hardly affects the cooling.

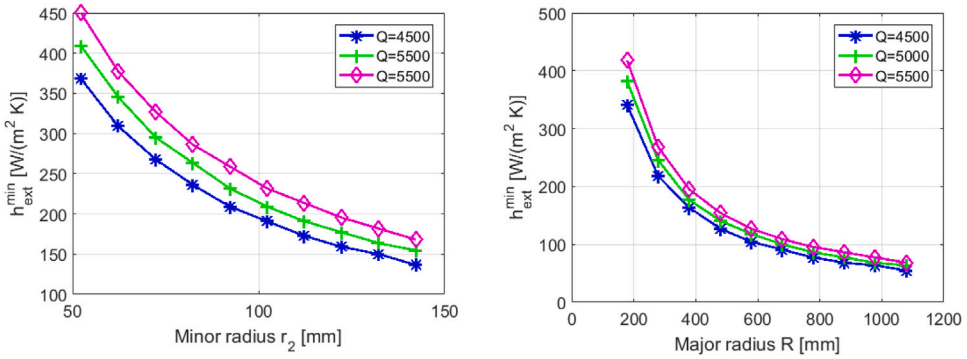

Fig. 8. Value of h_{ext}^{min} for the numerical experiments in Table 3 for different values of the heat flux Q (W) dissipated by the Litz wires. Left: Case 3, Right: Case 4.

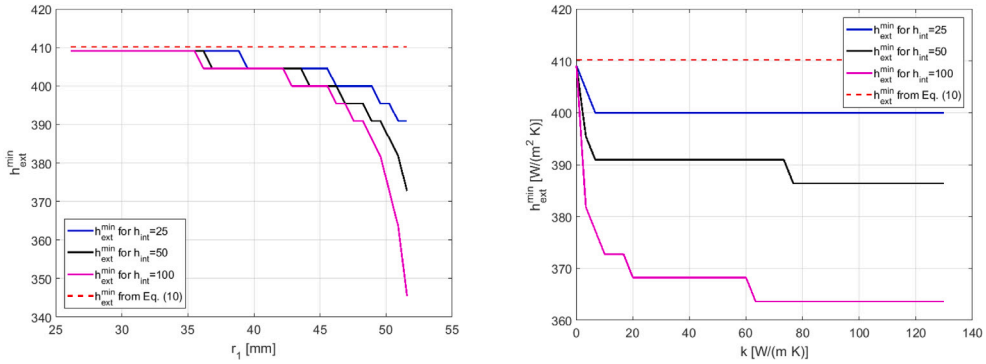

Fig. 9. Value of h_{ext}^{min}. Left: varying r_1. Right: $r_1 = 26.12$ and varying k, the thermal conductivity of the torus material.

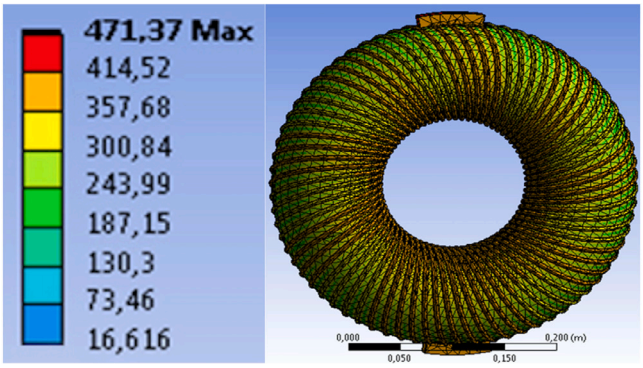

Fig. 10. The temperature rise of the coupler with natural convection (h_{ext} = 25 W m^{-2} K^{-1}) with $T_{ext} = 20$ °C.

In Fig. 8, we notice that h_{ext}^{min} decreases as the minor and major radius of the electromagnetic coupler increases, which is obvious because the larger the exchange surface, the easier the cooling. In both cases, when the radius (r_2 or R) is doubled, the value of the convective exchange coefficient h_{ext}^{min} required to maintain the PLA electromagnetic coupler at an acceptable temperature is halved (from a value of 400 W m^{-2} K^{-1} to a value close to 200 W m^{-2} K^{-1}).

We conclude this parametric optimization by computing the percentage error between the numerically optimized h_{ext}^{min} and the explicit one from (10), namely

$$100\frac{\max\left|h_{ext}^{min}-\frac{Q}{S_{ext}(60-T_{ext})}\right|}{\max\left|\frac{Q}{S_{ext}(60-T_{ext})}\right|},$$

Table 4
Percentage error between the numerically optimized h_{ext}^{min} and (10).

	$Q = 5500$ [W]	$Q = 5000$ [W]	$Q = 4500$ [W]
Case 1	0.6713%	0.5569%	0.7572%
Case 2	7.0652%	6.6612%	7.4020%
Case 3	0.9396%	1.0488%	1.2346%
Case 4	7.0652%	6.6612%	7.4020%

where the max is taken on each varying parameter according to the case considered. The results are shown in Table 4. Therefore, although the temperature distributions inside the torus for $h_{int} = 0$ (adiabatic wall) and $h_{int} > 0$ are very different, the numerical values of h_{ext}^{min} are actually very closed to the explicit value (10) except, for Cases 2–4.

It is worth noting that the explicit formula (10) does not depend on k, r_1 nor h_{int} and we thus now study the influence of these two remaining parameters on h_{ext}^{min}. Our numerical results are found with

$$Q = 5000\ [\mathrm{W}],\ T_{ext} = T_{int} = 300\ [\mathrm{K}],\ r2 = 52.25\ [\mathrm{mm}],\ R = 178.25\ [\mathrm{mm}],$$

with varying h_{int} from 25 to 100 W m^{-2} K^{-1}.

The numerical results can be found in Fig. 9. Both values diverge from each other if the inner heat transfer coefficient and the conductivity are larger and, in such cases, a smaller h_{ext}^{min} is obtained for the torus cooling.

From our numerical investigations we can conclude that formula (10) can be used to get h_{ext}^{min} if the inner heat transfer coefficient is small enough, and that in the other cases the choice of cooling by the interior of the torus makes it possible to reduce the value of the external heat transfer coefficient in a non-negligible way.

The heat transfer exchange coefficients for free or forced convection (internal and external) chosen correspond to realistic cases that can be obtained from correlations of the evolution of the Nusselt number for a flow of air outside the torus or for a flow of air or liquid inside the torus (case of a curved channel with a circular section) [10].

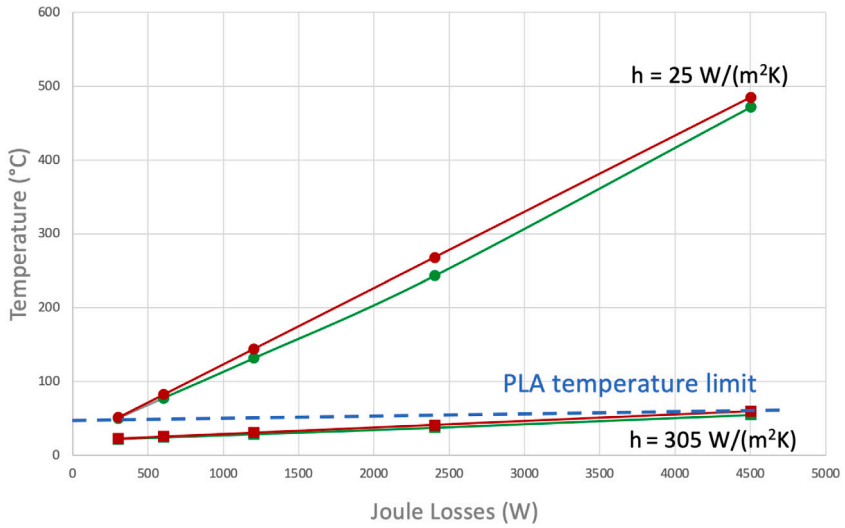

Fig. 11. Temperature's evolution of the electromagnetic coupler as a function of Joule losses and for natural convection with h = 25 W m^{-2} K^{-1} and forced convection with h = 305 W m^{-2} K^{-1}.

4. Cooling the torus with winding

In this section, we perform numerical simulations that take into account the wires to verify the mathematical model. The steady-state thermal analysis of the electromagnetic coupler was carried out using the commercial software ANSYS-Fluent. The geometry simulated includes the hollow PLA cable holder and the primary and secondary Litz wire windings. The diameter of a single strand of Litz wire in high-frequency applications is very small (a few tens of micrometers). Taking into account the depth of the skin effect requires substantial meshing and is time-consuming. Therefore, the method proposed by [18] to simulate the Litz wire is used. It consists in homogenizing the whole Litz bundle by finding its complex quantities. Each strand is replaced by an equivalent material represented by complex permeability and conductivity and then the whole bundle is homogenized with its equivalent complex quantities. The software takes as heat sources a primary power loss of 2.3 kW and a secondary power loss of 2.2 kW. In order to simplify these numerical simulations, the following assumptions are made:

- The ambient temperature is constant and is equal to 20 °C. It is also the initial temperature chosen for the simulation.
- There is no influence of the temperature rise on the thermal properties of materials (PLA and copper).
- Heat losses are constant and uniformly distributed in each turn of the Litz wires, which implies that the heat flux density is no longer homogeneous, as assumed in the previous study, but now depends on θ and ϕ.

Firstly, it is mandatory to determine the temperature rise in the system with natural convection. The cable holder and the windings have been meshed by tetrahedral volume elements generated automatically, then refined, adapted and optimized in order to obtain the best mesh which gives a good compromise between precision of results and calculation time. The mesh has 165,658 nodes and 80,163 elements, and a time-accurate thermal analysis is used for the solution procedure.

To obtain the following results, the Euler-explicit method was used with a step time of 0.5 s. Additionally, 8 h of CPU-time were needed using a PC-server with 8 processors (3.6 GHz processor and 64 GB RAM).

The temperature distribution is shown in Fig. 10 for a convective heat transfer coefficient of 25 W m^{-2} K^{-1}. The highest temperature in the electromagnetic coupler is the temperature of the winding, which is equal to 471.37 °C. From the mathematical model presented in

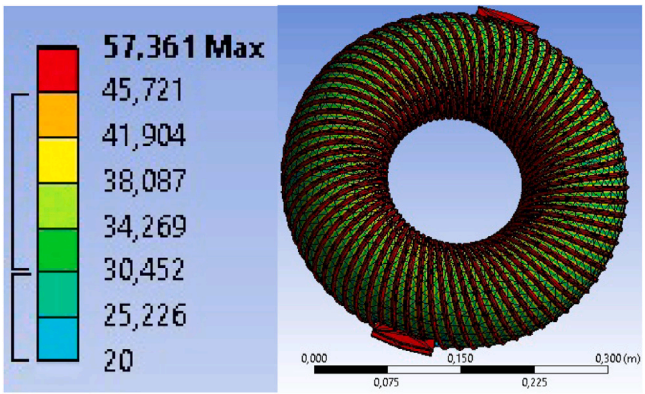

Fig. 12. The temperature rise of the coupler with forced convection (h_{ext} = 305 W m^{-2} K^{-1}) with T_{ext} = 20 °C.

Section 3.3, the temperature rise with natural convection was found to be 484.55 °C which means, that the difference between the two methods is only 2.8%.

The temperature reached is much higher than the limit temperature supported by the PLA material. As indicated in Fig. 6, it is therefore mandatory to introduce an efficient cooling system in order to avoid exceeding the operating temperature limit. Therefore, a convective heat transfer coefficient needs to be determined to consider the effect of the fluid on the solid. Generally, this coefficient can be provided through experimental tests. In our case, this coefficient is determined by using the approach in Section 3. According to the dimensions of the coupler and for heat losses of 4.5 kW, the calculated value for the external heat transfer coefficient is 305 W m^{-2} K^{-1} for the primary and secondary windings and the PLA cable holder.

Fig. 11 represents the temperature evolution of the coupler as a function of Joule losses for two values of the heat transfer coefficient. The red curve is the temperature rise obtained by using the mathematical model and the green curve is the result of the full numerical modeling. The results are very consistent: the difference between the two methods varies between 1.25% for low losses and 9.5% maximum for significant ones.

To enable the continuous functioning of the coupler without developing a cooling solution, maximum losses should not exceed 300 W, which means that only 1.3 kW can be transmitted from the primary

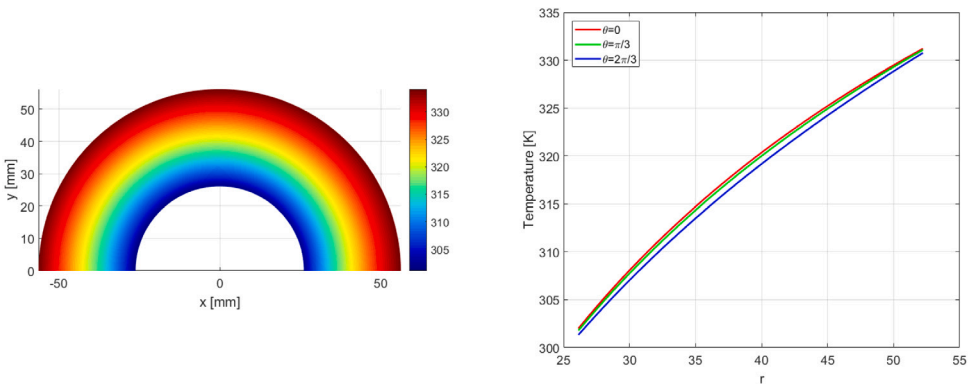

Fig. 13. The temperature rise of the coupler's loop as function of r (mm) with forced convection ($h_{\text{int}} = 25$, $h_{\text{ext}} = 305$ W m^{-2} K^{-1}) with $T_{\text{ext}} = T_{\text{int}} = 20$ °C.

Table 5
L^2 error between the numerical and the explicit solution for varying meshsize.

Meshsize τ	0.1414	0.02828	3.06204×10^{-5}
L^2-error	0.148168	3.06204×10^{-5}	4.82811×10^{-7}

to the secondary windings. This is at odds with the goal and ultimate application of the system. For this reason, the experimental test under the normal condition at a high-power level could not be conducted, mainly in order not to destroy the electromagnetic coupler and the power converters located upstream and downstream of the coupler.

Using a cooling system (with h = 305 W m^{-2} K^{-1}) will enable the coupler to work at high power, up to 200 kW, without exceeding the PLA temperature limit.

Fig. 12 represents the temperature field for the electromagnetic coupler. The maximum temperature reached in the primary and secondary windings is 57.36 °C, and in the PLA cable holder 38.08 °C. The heating of the coils is more intense than of the holder given their high thermal conductivity. In addition, the thermal limits of the different system components are respected.

Fig. 13 represents the temperature rise of the coupler's loop with forced convection using the simplified model from Section 3. For the same convective heat transfer coefficient, the maximum temperature reached is 332 K (59.95 °C). Although this value is equal to the limit temperature supported by the PLA, it does not present any danger of destroying the system.

5. Conclusion and perspectives

This paper presented two numerical approaches in order to study the cooling of a high-power toroidal electromagnetic coupler. The first methodology adopted estimates an approximate temperature distribution of the system by solving a 2D heat equation in poloidal coordinates and numerically optimizing the heat transfer coefficient without taking the Litz windings into account. The second approach considers the complex geometry of the coupler with windings and relies on 3D numerical modeling.

Both methods give results that are in good agreement. The maximum difference between the two methods used is about 9.5% only for the chosen parameters. This verifies the model presented in this paper and shows that it can be trusted when designing an electromagnetic coupler, with the consequence that complex, expensive CAD and CFD software, with time-consuming calculations, is not really required.

A CFD-type modeling will, however, be necessary when the choice of internal and/or external cooling solutions for the toroidal electromagnetic coupler is made. This numerical study allowed us to obtain the local convective exchange coefficients under cooling conditions. Furthermore, once the cooling solution is developed and the electromagnetic coupler is able to operate under normal conditions, experimental tests to evaluate the temperature rise with a high-power level will be performed, in order to validate the two developed methods.

Moreover, the parametric study showed that is very difficult to cool down the electromagnetic coupler using PLA material due to its low thermal conductivity and temperature limit. We believe that exchanging the PLA material for another, higher thermal conductive material (such as TC Poly) will allow the coupler to be cooled from inside, which will be a more effective and innovative solution.

Declaration of competing interest

The authors declare that they have no known competing financial interests or personal relationships that could have appeared to influence the work reported in this paper.

Acknowledgments

The authors are grateful to the French Ministry for Defense (Direction Générale de l'Armement) for its financial support for this work (RAPID CEMPER N° 172906093).

The authors would also like to thank members of the French company EFFITECH for their collaboration.

Appendix. Code verification for the thermal modeling

We proceed here with a validation of the code used to compute the value of $h_{\text{ext}}^{\min}$ To do this, we consider the following manufactured solution

$$T_{\text{exact}}(r,\theta) = ar + b,$$

with

$$a = -\frac{h_{\text{int}}(S_{\text{ext}}T_{\text{ext}}h_{\text{ext}} - S_{\text{ext}}T_{\text{int}}h_{\text{ext}} + Q)}{S_{\text{ext}}(h_{\text{ext}}h_{\text{int}}r_1 - h_{\text{ext}}h_{\text{int}}r_2 - h_{\text{ext}}k - h_{\text{int}}k)}$$

$$b = \frac{S_{\text{ext}}T_{\text{ext}}h_{\text{ext}}h_{\text{int}}r_1 - S_{\text{ext}}T_{\text{int}}h_{\text{ext}}h_{\text{int}}r_2 - S_{\text{ext}}T_{\text{ext}}h_{\text{ext}}k - S_{\text{ext}}T_{\text{int}}h_{\text{int}}k + Qh_{\text{int}}r_1 - Qk}{S_{\text{ext}}(h_{\text{ext}}h_{\text{int}}r_1 - h_{\text{ext}}h_{\text{int}}r_2 - h_{\text{ext}}k - h_{\text{int}}k)}.$$

One can then check that T_{exact} is the exact solution to (6)–(7) with

$$F = -\frac{(2r\cos(\theta) + R)a}{(r(R + r\cos(\theta)))}$$

as source term. The L^2 error defined as

$$\sqrt{\int_{r=0}^{1}\int_{\theta=0}^{2\pi}\left(\widetilde{T} - T_{\text{exact}}\right)^2\sqrt{g}\,dr\,d\theta},$$

can be found in Table 5. These results show the convergence of the numerical solution toward the exact one, thus validating the code.

The numerical simulations in Section 3.3 were all done using FreeFem ++ software [16] available at www.freefem.org. The code can be found at https://osur-devspot.univ-reunion.fr/phcocque/conduction_torus.

References

[1] M. Nicholas, D. Hall, Lessons learned on early electric vehicle fast-charging deployments, Int. Council Clean Transp. (2018) 54.

[2] F. Boudara, M. Rivaletto, L. Pecastaing, A. Silvestre de Ferron, S. Paquet, J.-P. Brasile, Design and development of high efficiency 150 kw very compact PLA core electromagnetic coupler for highly resonant power transfer technology, J. Electromagnetic Anal. Appl. 12 (09) (2020) 131.

[3] URBANLABS, Web site URBANLABS, technical Data sheet of the PLA, http://www.urbanlabs.co.in/products/pla-page.

[4] T. Leweke, M. Provansal, The flow behind rings: bluff body wakes without end effects, J. Fluid Mech. 288 (1995) 265–310, http://dx.doi.org/10.1017/S0022112095001145.

[5] Y. Inoue, S. Yamashita, M. Kumada, An experimental study on a wake of a torus using UVP monitor, Exp. Fluids 26 (1999) 197–207.

[6] M. Yovanovich, J. Culham, S. Lee, Natural convection from horizontal circular and square toroids and equivalent cylinders, J. Thermophys. Heat Transfer 11 (3) (1997) 415–422.

[7] N. Moshkin, J. Sompong, P. Suwannasri, Numerical study of flow and heat transfer from a torus placed in a uniform flow, J. Eng. Thermophys. 22 (2) (2013) 122–133, http://dx.doi.org/10.1134/S1810232813020045.

[8] O. Zeitoun, Numerical modeling of natural ocnvection heat transfer from a horizontal torus, Numer. Heat Transfer 65 (2014) http://dx.doi.org/10.1080/10407782.2013.875796.

[9] S. Berger, L. Talbot, L. Yao, Flow in curved pipes, Annu. Rev. Fluid Mech. 15 (1) (1983) 461–512, http://dx.doi.org/10.1146/annurev.fl.15.010183.002333, http://www.annualreviews.org/doi/abs/10.1146/annurev.fl.15.010183.002333.

[10] S. Vashith, V. Kumar, K. Nigam, A review on the potential applications of curved geometries in process industry, Ind. Eng. Chem. Res. 47 (10) (2008) 3291–3337.

[11] M. Ghobadi, Y. Muzychka, A review of heat transfer and pressure drop correlations for laminar flow in curved circular ducts, Heat Transf. Eng. 37 (10) (2016) 815–839.

[12] S. Wiesche, Transient heat conduction in a torus: theory and application, Heat Mass Transf. 38 (2001) 85–92.

[13] R. Alassar, M. Abushoshah, Heat conduction from donuts, Int. J. Mater. Mech. Manuf. 1 (2013) 126–130, http://dx.doi.org/10.7763/IJMMM.2013.V1.28.

[14] R. Alassar, M. Abushoshah, Cooling of a hot torus, J. Heat Transf. 138 (4) (2016).

[15] M. Fecko, Differential Geometry and Lie Groups for Physicists, Cambridge university press, 2006.

[16] F. Hecht, New development in freefem++, J. Numer. Math. 20 (3–4) (2012) 251–265, https://freefem.org/.

[17] H. Brezis, Functional Analysis, Sobolev Spaces and Partial Differential Equations, Springer Science & Business Media, 2010.

[18] M. Etemadrezaei, S.M. Lukic, Equivalent complex permeability and conductivity of litz wire in wireless power transfer systems, in: 2012 IEEE Energy Conversion Congress and Exposition (ECCE), IEEE, 2012, pp. 3833–3840.